The International Journal of Advanced Manufacturing Technology (2021) 112:833–843
https://doi.org/10.1007/s00170-020-06282-x

ORIGINAL ARTICLE

Modeling and fitting of an ultrasonic straight-blade cutting system

Ke Ma[1] · Jianfu Zhang[1,2] · Pingfa Feng[1,2,3] · Dingwen Yu[1] · Zhijun Wu[1]

Received: 24 April 2020 / Accepted: 19 October 2020 / Published online: 24 November 2020

Abstract
Ultrasonic straight-blade tool is one type of effective tool for processing Nomex composites. As a system part, the ultrasonic tool, directly contacting the workpiece and providing the vibration, is an important acoustic element alongside the cutter. And the resonant frequency of ultrasonic processing systems, a key parameter of the vibration performance, is greatly influenced by the straight-blade tool changes when connected to the ultrasonic system. In the present paper, a mathematical model for calculating the resonant frequency was established for the ultrasonic straight-blade tools with variable cross-sectional areas. The relationship between the parameters of the straight-blade tool and the resonant frequency, as well as between the force and the vibration of the ultrasonic system, were presented and utilized to calculate the system resonant frequency change and the corrected horn value to hold the frequency. To solve the vibration equations, they were refined by fitting a trigonometric function combination. The errors of the vibration equations and the fitting were analyzed, showing the applicable scope of the vibration equations. According to the model and the common ultrasonic straight-blade tool sizes, four tools were manufactured for verification experiments. Results showed that the presented model could be well matched with the actual value.

Keywords Ultrasonic straight-blade tool · Vibration model · Resonant design · Error analysis

1 Introduction

The Nomex honeycomb composites have been widely applied in the aviation, aerospace, defense, and automotive field due to their low density, high specific strength, high specific stiffness, and good thermal insulation [1–3]. However, Nomex honeycomb composite has poor processability because of its special properties, such as anisotropy, brittleness, and easy deformation. Nomex honeycomb composite processing defects caused during the conventional processing techniques, such as high-speed milling, greatly affected its application. In traditional milling, the high-speed rotating tools smash the Nomex honeycomb composites, causing problems such as cell collapse, large dust high tool wear, and low surface quality, whereas Nomex honeycomb composite ultrasonic processing provides an ideal processing effect [4, 5]. The ultrasonic straight-blade tools cut Nomex honeycomb composites into pieces like a saw under the action of ultrasound, which helps to improve the processing quality of Nomex honeycomb composites. Ultrasonic machining has advantages such as low tool wear, high efficiency, high surface quality, low processing defects, and no processing pollution [6, 7].

Ultrasonic machining is widely utilized to process brittle materials [8]. Ultrasonic straight-blade cutting is a common method for processing Nomex honeycomb composites. Studies have developed ultrasonic processing systems and explored the ultrasonic cutting processing technology for Nomex honeycomb composite [6, 9, 10]. Beyond cutting Nomex composites, the straight-blade tool is also used to process floppy, brittle, and ductile materials, such as plastic, rubber, and polymer [11]. In recent years, the ultrasonic straight-blade tool is also utilized as medical devices, such as the sonic scalpel and osteotome.

The ultrasonic straight-blade tool is generally applied in rough cutting of Nomex honeycomb composites to remove large volume of material from workpiece [12]. In ultrasonic processing, the system resonant frequency is an important parameter determining the system resonance result, the cutting

✉ Jianfu Zhang
zhjf@tsinghua.edu.cn

[1] Beijing Key Lab of Precision/Ultra-precision Manufacturing Equipments and Control, Department of Mechanical Engineering, Tsinghua University, Beijing 100084, China

[2] State Key Laboratory of Tribology, Department of Mechanical Engineering, Tsinghua University, Beijing 100084, China

[3] Division of Advanced Manufacturing, Tsinghua Shenzhen International Graduate School, Tsinghua University, Shenzhen 518055, China

effect, and the work performance of each part. Some studies proposed the ultrasound-related methods for designing the resonant frequency of the transducers and horns [13–17], while many researchers studied the effects of temperature, atmospheric moisture, cutting parameters, and the transducer material types (piezo-ceramics, giant magnetostrictive material) on the resonant frequency and the effective frequency bandwidth of the ultrasonic system [18–20]. To hold a stable resonant frequency for the ultrasonic system during processing, some studies propose resonance tracking methods [21, 22], and some studies provide instruments to detect and correct the ultrasonic system resonant frequencies [23]. Every part of the ultrasonic system influences the system resonant frequency due to their sizes in the vibration friction. The normal ultrasonic cutting tools, such as the disc cutter, the milling cutter, and turning tool, are short in the longitudinal vibration friction direction. The tool contact length is usually no more than 10 mm. Therefore, the influences of these cutting tools on the resonant frequency and amplitude are rarely considered.

However, a straight-blade tool approximately 40 mm in length in the vibration friction direction has great influences on the ultrasonic system resonant frequency. Wu [24] conducted simulations on the straight-blade tool to investigate the influence of ultrasonic resonance from the tool shape, length, and thickness. Results showed that the tool thickness was negatively correlated with the amplitude and had less influence on the resonant frequency, while the tool length had more influence. Zhou [25] deduced the ultrasonic system with the back cover, the piezoelectric ceramics, the front cover, the horn, and the straight tool to achieve the complete resonance equation in the longitudinal vibration. The system frequency was calculated via the parameters of each structure. Zhang [26] derived the ultrasonic tool vibration equation with rectangular shape through the horn design and simplified the equation via the Ritz method, which is helpful to the ultrasonic tool design with a constant cross-sectional area. Hu [27] proposed an approximation model for ultrasonic systems and investigated an ultrasonic component design method based on the SVR algorithm. The approximate model was calculated via this method based on setting the parameters within a certain range and facilitating individual component designs under fuzzy design conditions.

In the studies mentioned above, they focus on the relationship between ultrasonic tools and resonant frequency. Some problems remain to be solved to get better performance and efficiency out of the ultrasonic system. The current methods for reversing the geometrical parameters of each structure through design requirements and providing a method to design common straight-blade tools with variable cross-sectional areas are defective. And, the method for maintaining the resonant frequency when installing different straight-blade tools for the same ultrasonic system is not raised.

In the present paper, the equations of the ultrasonic straight-blade tool with variable cross sections were proposed then simplified by fitting for the resonance equation. The equations revealed the influence of various parameters of the common straight-blade tools on the resonant frequency, which is beneficial to designing ultrasonic straight-blade tools. The reliability of the theoretical equations was verified via the experiments.

2 Modeling of triangular ultrasonic straight-blade tools

The ultrasonic straight-blade tool is commonly used for the V-shaped rough machining of Nomex honeycomb composites. Figure 1 shows that an ultrasonic straight-blade tool system consists of a power supply, control circuit, transducer, horn, and the straight-blade tool. The power supply generates ultrasonic electric signal. The transducer turns the electric signal from the power supply into ultrasonic mechanical vibration. And the horn amplifies the vibration, which drives the GMM to produce ultrasonic strain along the axis. The horn realizes the transmission and amplification of ultrasonic vibration along the axis of the blade tool.

Figure 2 shows the straight-blade tool is normally used for rough-machining the Nomex honeycomb materials. Because the chip shapes and machined surfaces are V-shaped, this method is also called V-shaped cutting.

In an ultrasonic system, every part with a length in the direction of the wave transmission changed the antinode position, thereby changing the system resonant frequency. The effect on the system resonant frequency was positively related to the dimension in the transmission direction of the ultrasonic system parts.

The normal straight-blade tool area changed linearly with the axis which led to more complex vibration equations, and it was different from the equal cross-sectional area of the rectangular straight-blade tools or the secondary area of the circular section horns.

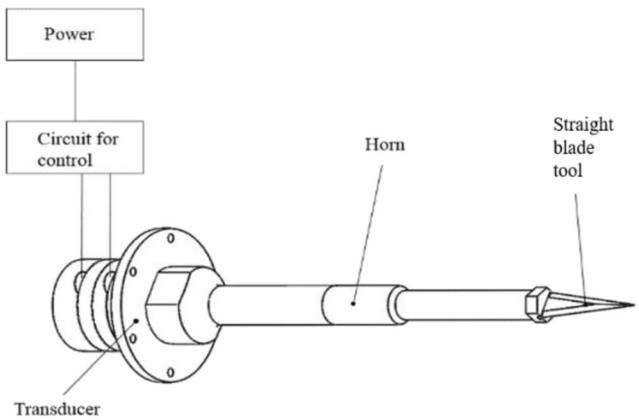

Fig. 1 Ultrasonic straight-blade tool system

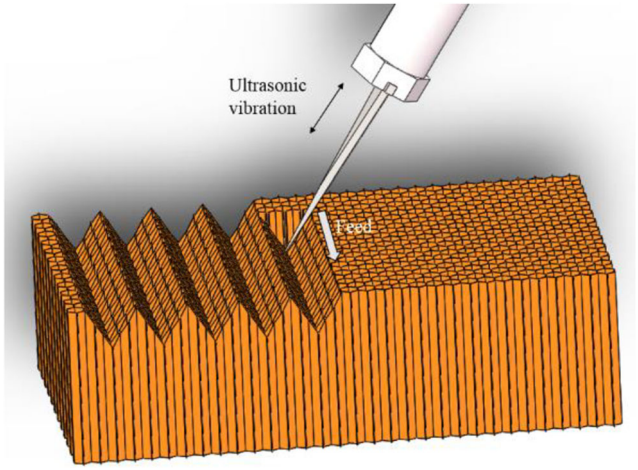

Fig. 2 The V-shaped cutting

2.1 Vibration model of triangular straight-blade tools

Figure 3 shows a typical triangular ultrasonic straight-blade tool. The main structure parameters of the straight-blade tool were the tool height $m(x_1)$, length l_1, thickness n, angle of the tool nose α, and draft angle β.

Supposing the distance from the tool tip was x_1, the cross-sectional area of the tool was:

$$S(x_1) = \left(m(x_1) - \frac{n}{2\tan\frac{\beta}{2}} \right) n = S(l_1)\frac{x_1}{l} \tag{1}$$

$S(l_1)$ was the cross-sectional area on the left end of the tool. To get a longitudinal vibration, the model considered one-dimensional vibrators when the maximum circumferential dimension of the cross section of the straight-blade tool was less than one-quarter wavelength. The vibration equation of the one-dimensional longitudinal vibrating rod was [28].

$$\varepsilon = \frac{F}{S(x_1)} = E\frac{\partial u}{\partial x_1} \tag{2}$$

where ε was the strain, F was the force, and u was the displacement function related to the tool position and time. For a continuum of variable cross section, there was:

$$\frac{\partial^2 u}{\partial x_1^2} + \frac{1}{S(x_1)}\frac{\partial S(x_1)}{\partial x_1}\frac{\partial u}{\partial x_1} = \frac{1}{C^2}\frac{\partial^2 u}{\partial t^2} \tag{3}$$

where t was the time, substitute (1) into (3):

$$\frac{\partial^2 u}{\partial x_1^2} + \frac{1}{x_1}\frac{\partial u}{\partial x_1} = \frac{1}{C^2}\frac{\partial^2 u}{\partial t^2} \tag{4}$$

Assuming $u(x_1,t) = v(x_1)q(t)$ was usually an effective way to solve this equation, where $v(x_1)$ was the vibration speed relevant to x_1, where $v(x_1)$ is a variable with unit of "m/s" and only related to x_1, and $q(t)$ was a variable with unit of "s" influenced by only t, (4) was simplified to:

$$\frac{v''(x_1) + \frac{v'(x_1)}{x_1}}{v(x_1)} = \frac{1}{C^2}\frac{\ddot{q}(t)}{q(t)} \tag{5}$$

In (5), there was only one variable on each side, and the variables were different, so the values of both sides were constant. The constant was recorded as y^2.

$$\frac{d^2 v}{dx_1^2} + \frac{1}{x_1}\frac{dv}{dx_1} + y^2 v = 0 \tag{6}$$

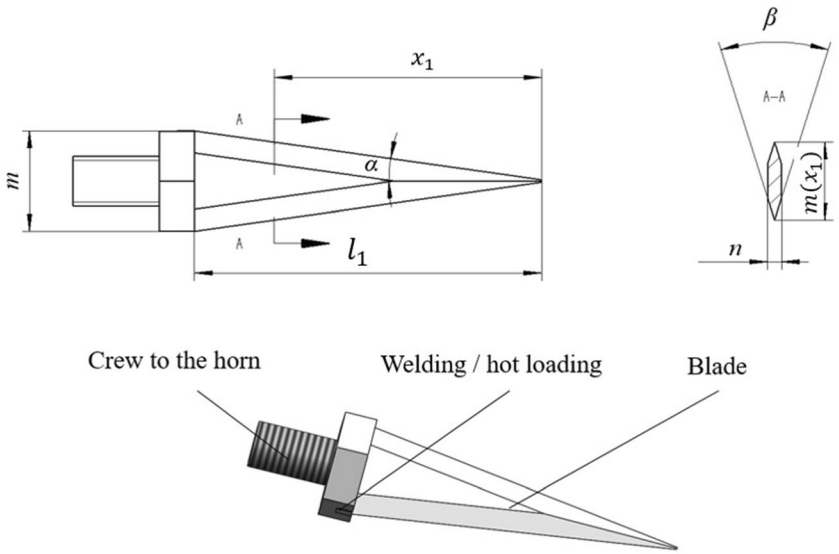

Fig. 3 Structure parameters of a triangular straight-blade tool

There was no elementary analytical solution for this equation, and its analytical solution needed to be represented by the Bessel function of the first order and the Neumann function of the first order. The solution of (6) was (7):

$$v_t(z_t) = c_{t1}J_0(z_t) + c_{t2}Y_0(z_t) \tag{7}$$

where k was the wave number and $z_t = kx_1$ was dimensionless, indicating the position of the z_t wavelength from the tool tip.c_{t1} and c_{t2} were constant in m/s. The curve $v_t(z_t)/v_{ti}$ vs. z_t is shown in Fig. 4, $v_t(z_t)/v_{ti}$ was the ratio of the input vibration speed v_{ti} to the vibration speed $v_t(z_t)$ at z_t wavelength positions from the tool tip.

The force at the section at z_t wavelength positions from the tool tip was:

$$F_t(z_t) = -j\rho CS(x_1)\frac{dv_t}{dx_1} = -j\rho kcS\left(\frac{Z_t}{k}\right)[-c_{t1}J_1(z_t) - c_{t2}Y_1(z_t)] \tag{8}$$

where ρ was the density and C was the speed of sound of the tool material. The boundary conditions were utilized to obtain the coefficients c_{t1} and c_{t2}. On the right end of the tool, a line of 2 mm existed instead of a point to increase the tool strength, so the minimum value of x_1 was not 0. When the tool length was l_1, the minimum value of x_1 was $\delta = f(l_1)$, and a small amount of that tended to 0. Based on the speed of sound in steel and the frequency of 20 kHz, the boundary conditions were:

$$\begin{aligned} v_t(k\delta) &= v_{to} \\ v_t(kl_1 + k\delta) &= v_{ti} \\ F_t(k\delta) &= v_{to}Z_{to} \\ F_t(kl_1 + k\delta) &= v_{ti}Z_{ti} \end{aligned} \tag{9}$$

where the first subscript t represented the straight-blade tool and the second subscript i represented the physical quantity at the left end of the knife while o for these on the right end. v was the vibration velocity of the corresponding section and varied with the cross-sectional area. F was the tensile force on the cross section and Z was the acoustic impedance. The output impedance Z_{to} was regarded as 0 and v_{ti} was the horn output vibration velocity.

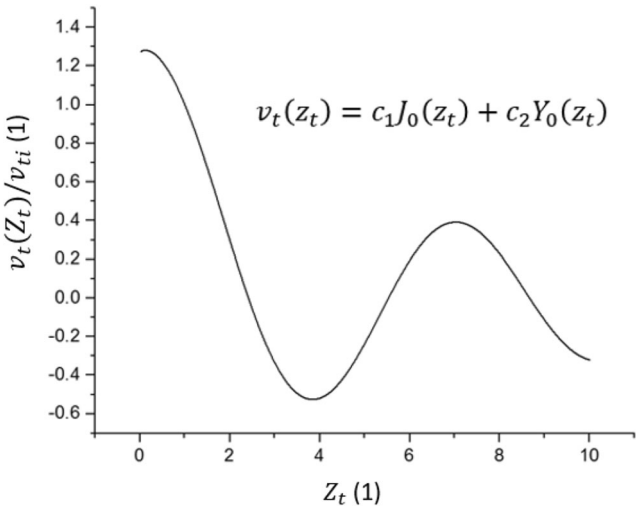

Fig. 4 The correlation curve between $v_t(z_t)/v_{ti}$ and z_t

2.2 Fitting of theoretical models

Since the Bessel functions are complex form and not conducive to the solution of stress, vibration velocity, and resonance equation, it was assumed that the analytical solution could be fitted with the elementary function. According to the vibration mechanics, the output was in the form of a trigonometric function when the input vibration was a trigonometric function. On the other hand, the tool was a continuum, so the energy passing through each section was consistent while the vibration remained stable, as shown in Fig. 5.

The vibration energy E_k through the arbitrary cross section was constant:

$$\begin{aligned} E_k &= \int dE_k = \int \frac{1}{2}v_t(z_t)^2 dm = \int \frac{1}{2}\rho S(x_1)(v_t(z_t))^2 dx_1 \\ &= \int \frac{1}{2}C_s\rho x_1(v_t(z_t))^2 dx_1 \end{aligned} \tag{10}$$

where ρ was the density of the material of the tool, m was the mass, and C_s was a constant.

$$\frac{1}{2}C_s\rho k z_t(v_t(z_t))^2 = const \tag{11}$$

Equation (11) assumed that the magnitude of the solution above $v_t(z_t)$ was proportional to $\frac{1}{\sqrt{z_t}}$ and appeared as a sine wave form. The analytical solution was fitted by $\frac{A\sin z_t + B\cos z_t}{\sqrt{z_t}}$. The absolute value of the integral from the input end of the tool to the output was taken as a reference to control the fitting function accuracy, $z_t = \delta/k$ to $z_t = (l_1+\delta)/k$:

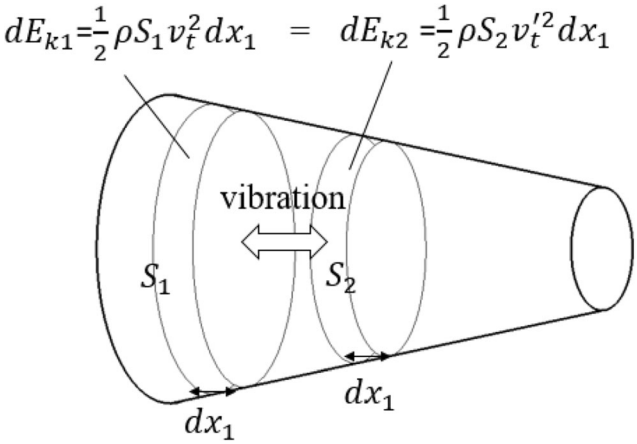

Fig. 5 Vibration energy of a continuum

$$\min\left(\int_{\delta/k}^{(l_1+\delta)/k}\left|c_{t1}J_0(z_t)+c_{t2}Y_0(z_t)-\frac{A\sin z_t+B\cos z_t}{\sqrt{z_t}}\right|dz_t\right) \tag{12}$$

As shown in Fig. 6, the fitted result was close to the analytical solution.

The vibration speed and the force on the section of the tool could be represented by (13):

$$\begin{aligned} v_t(z_t) &= v_{ti}\frac{A\sin z_t+B\cos z_t}{\sqrt{z_t}} \\ F_t(z_t) &= -j\rho cS(x_1)\frac{dv_t}{dx_1} = -j\rho cS(x_1)v_{ti}\left[A\left(\frac{k\cos kx_1}{\sqrt{kx_1}}-\frac{\sin kx_1}{2x_1\sqrt{kx_1}}\right)-B\left(\frac{k\sin kx_1}{\sqrt{kx_1}}-\frac{\cos kx_1}{2x_1\sqrt{kx_1}}\right)\right] \\ &= -jk\rho cS\left(\frac{z_t}{k}\right)v_{ti}\left[A\left(\frac{\cos z_t}{\sqrt{z_t}}-\frac{\sin z_t}{2z_t\sqrt{z_t}}\right)-B\left(\frac{\sin z_t}{\sqrt{z_t}}-\frac{\cos z_t}{2z_t\sqrt{z_t}}\right)\right] \end{aligned} \tag{13}$$

The ratio of the normal stress to the input normal stress in the sections of the straight-blade tool was obtained from the model proposed in the manuscript. Figure 7 shows the curve of the ratio to the cross-sectional coordinates that were obtained by ANSYS simulation and were made with the error. The data calculated by the model was in line with that in the simulation, especially for those near the boundaries.

2.3 Coupling model of tool and horn

Horns tend to be easy to remove when compared to ultrasonic transducers. Therefore, the coupling equation between the horn and the straight-blade tool was calculated for designing them together in a definite resonant frequency.

Figure 8 shows the horn, with a length of l_2, was a part with a cross-sectional area that was always πr^2. Substituting $S_h(x) = \pi r^2$ into (2), the vibration velocity equation was obtained as $v_h = C_h\sin kx_2 + D_h\cos kx_2$.

The boundary conditions of the horn were:

$$v_h(0) = v_{ti}, v_h(l_2) = 0, F_h(0) = F_t(l_1) \tag{14}$$

Taking the boundary conditions into $v_h = C_h\sin kx + D_h\cos kx$, the constants C_h and D_h could yield:

$$\begin{aligned} D_h = v_{ti}, C_h &= -cot(kl_2)v_{ti}, \\ v_h &= v_{ti}(-cot(kl_2)sinkx_2 + v_{ti}coskx_2) \end{aligned} \tag{15}$$

Considering (14), (15), and (13), the coupled vibration frequency equation of the horn and the tool was calculated as:

$$\frac{-2Akl_1+A\tan kl_1+2Bkl_1\tan kl_1+B}{2kl_1\cot kl_2\sqrt{kl_1}\cos kl_1} = \frac{\pi r^2}{2mn-\frac{n^2}{2\tan 0.5\beta}} \tag{16}$$

Equation (16) describes the relationship between the resonant frequency of the horn with the straight-blade tool and various tool parameters. This resonant frequency was the resonant frequency of the entire ultrasound system if the resonant frequency of the transducer was also designed in the same basic value. There was $\cot kl_2$ on the denominator in the left side of (16), which was infinite with constant l_2. For an ultrasonic system designed in a basic frequency without the straight-blade tool, the resonant frequency of the system must change regardless of any tool parameter after installing the tool. To keep the basic resonant frequency constant, the horn length should be corrected. The corrected horn length could be calculated with (16), substituting parameters such as frequency and tool length.

Figure 9 shows the relationship between the various parameters of the straight-blade tool and the resonant frequency of the ultrasonic system, in which each parameter varied from 0.75 to 1.25 times the basic value. The tool length had the greatest influence on the system resonant frequency, while the influence of the thickness and the length of the end were small, and the influence of the cutting edge angle was smallest. In fact, these parameters of the tools will greatly affect other cutting performances, such as the tool strength and degree of sharpness. Therefore, the length of the straight-blade tool was studied and the coupling model of tool

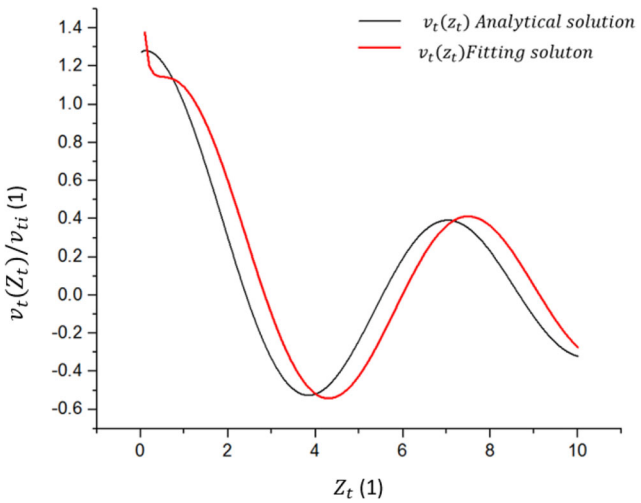

Fig. 6 The fitting solution

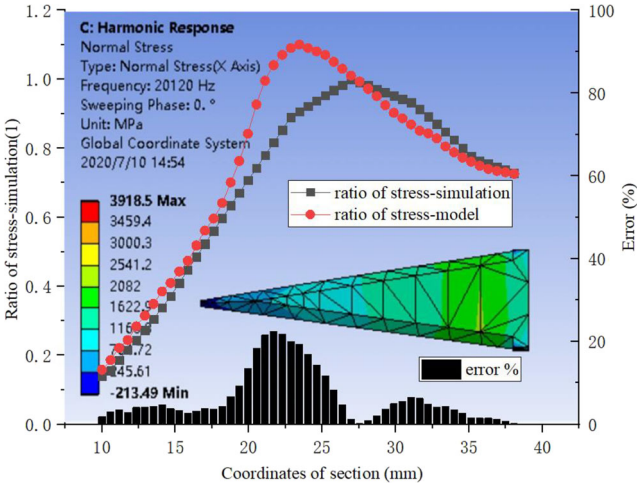

Fig. 7 Curve for the ratio of stress and the coordinates of the section

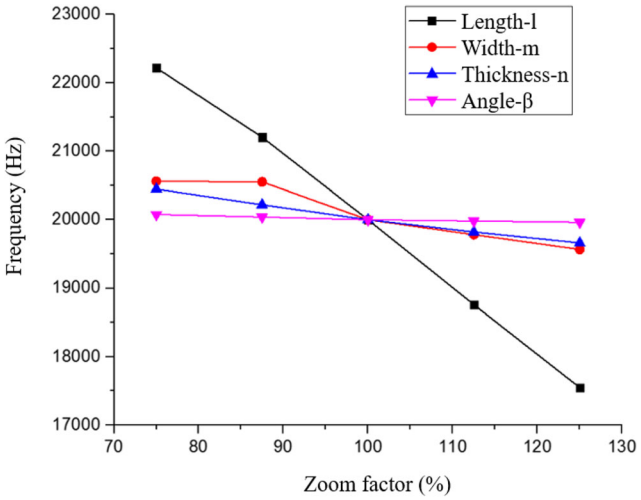

Fig. 9 Relationship between the parameters and the resonant frequency

and horn was utilized to calculate the resonant frequency of the entire system. Furthermore, ultrasound systems of a given frequency with the straight-blade tool and the horn design method were proposed for the coupling model.

3 Discussion of the models

Since the model boundary conditions and the fitted interval were not always the same with the actual values, the presented model has systematic errors. In (9), k was not a constant but a wave number related to the resonant frequency. Therefore, for the model calculated with the basic resonant frequency of f, when the resonant frequency of the system was not f, the boundary conditions of the model were incorrect, leading to an error.

Considering the error, v_t and F_t in (9) should be changed to:

$$v_t((k+\varepsilon)l_1+(k+\varepsilon)\delta)=v_t(kl_1+\varepsilon l_1+k\delta+\varepsilon\delta)=v_{ti} \tag{17}$$

$$F_t((k+\varepsilon)\delta)=F_t(k\delta+\varepsilon\delta)=v_{to}Z_{to}=0 \tag{18}$$

Among these, ε and δ were low-grade, so $\varepsilon\delta$ was negligible as a high-order small one. Therefore, the error of (18) was small and the proportional relationship between c_1 and c_2 obtained by the equation was accurate. The main source of error in (17) was from εl_1, which was a positive correlation with ε. Then, when the input frequency of the model deviated from the basic value 20 kHz, the model had the system error, so that c_1 and c_2 were proportionally enlarged or reduced. ε was a small amount below zero, so that the left end of the model did not coincide with the actual left-most end, shifting to the right, and the theoretical input vibration velocity v_{ti} was smaller than the actual vibration velocity v_{ti}' of the section. The abrupt surface of the cross-sectional area was the left end of the tool, and the vibration velocity was continuously changed in the tool segment. The error amplified c_1 and c_2, denoted as $v_{ti}=v_{ti}'\cdot k_{ti}=v_{ti}'\cdot(1+f(\varepsilon))$. c_1 and c_2 were also scaled up by $1+f(\varepsilon)$ times. This means that when $\varepsilon=0$, there was no systematic error. Figure 10 shows that while $\varepsilon<0$, c_1 and c_2 were proportionally magnified but the error changed continuously. If $\varepsilon>0$, c_1 and c_2 were scaled down and the cross-sectional area could be changed suddenly; a large error would be caused.

During the fitting process, the change of k also caused errors. In (16), the values of A and B were mainly affected by the length of the tool, but, simultaneously, the input frequency k slightly affected the value of A and B. When the value of k changed, the fitted region (δ/k $(l_1+\delta)/k$) was not exactly the same as the original function area. When the k became smaller, the lower limit value δ/k was smaller than the minimum value of the fitting domain, while the maximum value was still in the fitting domain. When the k became larger, the upper limit value

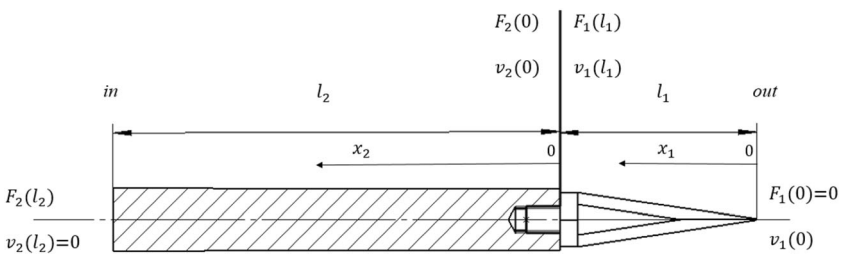

Fig. 8 Boundary conditions of the tool and the horn

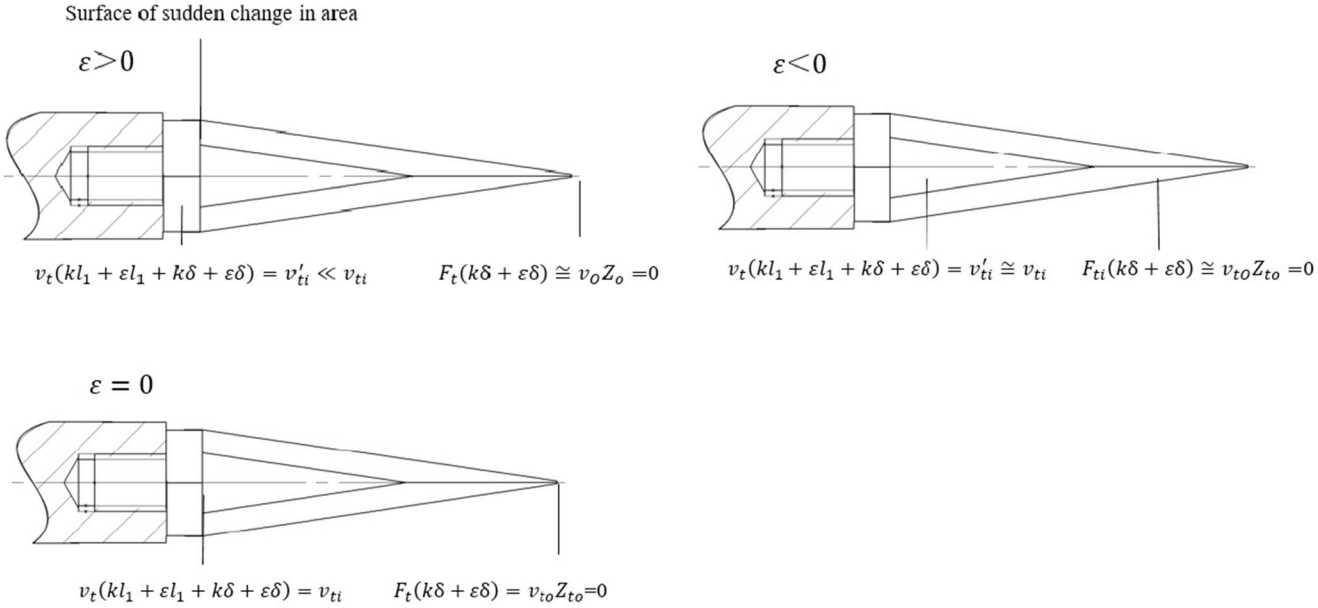

Fig. 10 Errors of the boundary conditions

$kl_1 + k\delta$ was bigger than the fitting. The maximum value of the domain was large, and the minimum was within the fitted domain. Among them, since δ itself was small, but $l_1+\delta$ was non-ignorable, k had little effect on the fitting when k became smaller, yet the fitting domain error and the original function were larger when k became larger. The change of k was the main source of systematic error. Transducers and ultrasonic power supplies were generally inconvenient parts of an ultrasonic system, so the coupling model proposed in this paper only included horns and straight-blade tools. The calculation of the model did not include the transducer, which would also cause errors between the actual resonant frequency and the calculated value if the actual resonant frequency was not the basic frequency.

According to the analysis above, the systematic error occurred only when the system resonant frequency changed. Therefore, the model calculated at the basic frequency of f without the tool could not accurately predict the system resonant frequency after installing the tool. When the tool length was larger, the value of k and the error were also higher. When the tool length was not correctly designed with the straight-blade tool, it may have a large deviation from the actual value. On the contrary, no systematic error existed for the horn design with the tool. The model was reliable when utilized to design a system at a determined resonant frequency or to design a new horn for an existing system to change its resonant frequency. On the other hand, when the model was utilized to calculate the system resonant frequency, the calculation results were more accurate with the smaller frequency variation range. If the frequency varied widely, the resonant frequency calculated by the model should only be utilized as a qualitative reference.

According to the model, the resonant frequency must change when there was force on the straight-blade tool in the actual processing. The model could be utilized to calculate the resonant frequency of the system subjected to external forces (only for axial forces), but it was of little significance unless the cutting force was constant and only utilized for the axial force. In an ideal situation, the external force on the tool could be obtained via a dynamometer and substituted into (9) to calculate a new model for calculating the system resonance frequency. In the process of measuring force, calculating the model, calculating and inputting new resonance frequencies into the system, the tool kept feeding and made the situation change faster than the processing.

Frequency tracking was more effective than utilizing the model to calculate the system frequency in cutting. The cutting force for processing Nomex honeycomb composites was only 1–10 N, and the change of resonance frequency was within 50 Hz. Based on the relationships among the dynamic resistance, impedance phase, and resonant frequency of the ultrasonic system, many methods such as the in-phase method and maximum-current method were utilized to track the resonance frequency automatically in real time when processing. Usually, a processor that collects and calculates the real-time resonance frequency was installed on the ultrasonic power source to complete frequency tracking. For example, for the in-phase method, when the system received an external force in actual processing, the resonance frequency changed, and the processor detected that the current and voltage output by the power supply had a phase difference. Then, the processor adjusted the output frequency according to the phase difference so that the current had the same phase with voltage, making the system working at the changed resonance frequency. These methods, changing

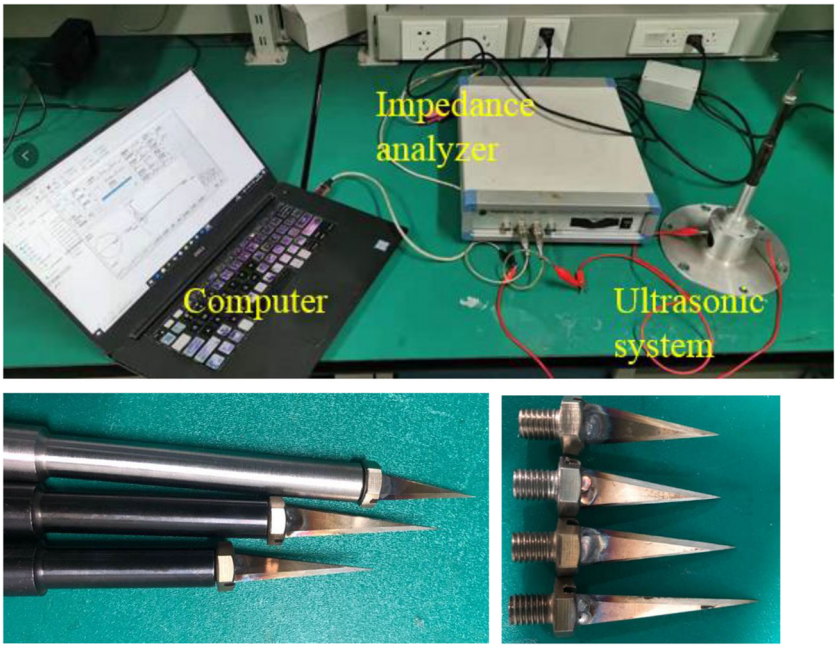

Fig. 11 The experiment of the straight tools

the input frequency of the system to the actual resonance frequency within 50 ms when the system was subjected to an external force, were more effective than utilizing this model to calculate the frequency.

4 Experiments and verification

An experimental system was built to measure the resonant frequency of the systems, as shown in Fig. 11. It was composed of an impedance analyzer, straight-blade tool ultrasonic system, and analysis software. The impedance analyzer was utilized to measure the resonant frequency of the ultrasonic system with a frequency accuracy of ± 0.005% and the software processed and displayed the frequency.

According to the sizes of the common ultrasonic straight-blade tools, four tools with lengths of 30 mm, 35 mm, 40 mm, and 45 mm were selected for the experiment. Without the straight-blade tool, the basic horn length was 74 mm with the basic resonant frequency of 20 kHz. First, the coupling models of different tools and the basic horn were established according to the method proposed in the present paper, and the parameters of the models were shown in Table 2. These models were then utilized to calculate the resonance frequencies of the ultrasonic systems, including basic horns with a length of 74 mm and straight-blade tools in different lengths. Finally, these models were utilized to calculate the corrected horn length suiting different straight-blade tools to maintain the resonant frequency of 20 kHz, as shown in Table 1. Figure 11 shows the ultrasonic transducers and ultrasonic horns with a resonant frequency of 20 kHz, corrected horn lengths, and the straight-blade tools with the fabricated lengths above.

The resonance frequencies of the ultrasonic systems with 74 mm long horns and straight-blade tools of four different lengths were measured and shown in Table 3, and the frequency of the ultrasonic systems with corrected horns and the same tools are measured as shown in Table 2.

A model which simplified the straight-blade tool geometry to a rectangular shape with a constant cross section (c

Table 1 Parameters of the couping model and the experiment

Length of the tool l_1 (mm)	Model parameters				Basic horn l ength l_2 (mm)	Corrected horn length l_2 (mm)
	c_1	c_2	A	B		
30	1.16	0.015	1.039	0.301	74	72
35	1.233	0.021	1.050	0.317		68
40	1.308	0.015	1.083	0.330		63
45	1.422	0.039	1.101	0.400		48

Table 2 Frequency comparison and error

Length of the tool l_1 (mm)	System frequency (Hz) (with basic horn)		Error (%)	System frequency (Hz) (with corrected horn)		Error (%)
	Theoretical value	Experimental value		Theoretical value	Experimental value	
30	19,560	19,225	1.7	20,000	20,335	1.7
35	18,910	18,212	3.8		19,890	0.6
40	18,184	17,308	5.1		20,062	0.3
45	16,940	15,283	10.8		20,480	2.4

Table 3 Compared with c model and variable cross-section model (v model)

Length of the tool l_1(mm)	System frequncy with basic horn(Hz)			Error(%)		Corrected horn length l_2(mm)	
	Experiment value	c model	v model	c model	v model	c model	v model
30	19225	18908	19560	1.7%	1.7%	70	72
35	18212	18681	18910	2.6%	3.8%	69	68
40	17308	18428	18184	6.4%	5.1%	67	63
45	15283	18143	16940	18.7%	10.1%	66	48

model) was established and compared with the model proposed in the present manuscript. The coupled vibration frequency equation of the horn and the tool with c model was $(Z_t/Z_h)\tan(kl_1)\tan(kl_2) = 1$. As shown in Table 3, the frequencies with the basic horn utilizing different straight-blade tools and the corrected horn lengths with these tools are calculated by the constant model.

For the system with straight-blade tools of different lengths, the theoretical and experimental values of the system resonant frequency with uncorrected and corrected horn length are shown in Fig. 12, and the same data of the c model are also shown in Fig. 12. In Fig. 12, "f-basic-e" means the resonant frequency measured in the experiment with the basic horn, "f" means the frequency, "basic" means the basic horn, "corrected" means the corrected horn, "v" means the v model data, "c" means the c model data, and "e" means the experimental data.

For the c model, the tool shape was treated as a rectangle, and the tool influence was reduced, which made the calculated frequency change little with the tool length change. As the tool length increased, the error of calculation data greatly increased. When the tool length was 35 mm or less, the calculated values of the c model and the v model were similar, while the error of the c model was far higher than that of the v model when the tool length was 40 mm or 45 mm. For the v model, in the data of the systems with the basic horn, the experimental value had a systematic error with the theoretical value, and the farther the frequency deviated from the basic resonant frequency, the larger the error was. When the frequency of the system deviated from 4 kHz, the error was about 10%, making the quantitative value lost. But a model based in basic frequency could be utilized to calculate whether the resonant frequency of the system increased or decreased with different straight-blade tools. The result was in line with the analysis of the previous section.

On the other hand, the resonant frequencies of the systems with corrected horns were in line with the experimental results and had few errors (less than 2.5%), which mainly came from the actual material parameters not being completely consistent with the theoretical values and the joint surface. The result was consistent with the conclusions drawn from the error analysis, and the model was accurate to design the ultrasonic straight cutting system in a given resonant frequency.

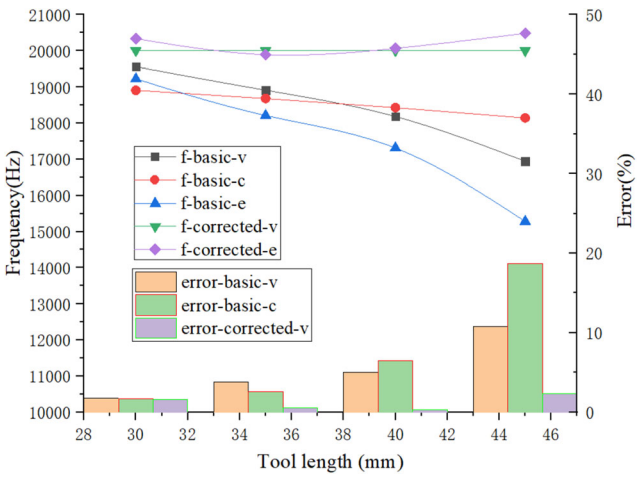

Fig. 12 Frequencies and errors of different models and horns

5 Conclusion

To solve the problem of the resonant frequency design for the ultrasonic straight-blade tool, the vibration model of the ultrasonic straight-blade tool with variable cross-sectional area was established based on the vibration theory and the equations of the vibration system were then presented by combining trigonometric functions. Results showed that the resonance frequencies could be well matched with the theoretical values. This provided ideas for the analysis of other ultrasonic structures with variable sectional areas. The following conclusions were drawn:

(1) The vibration model of the ultrasonic straight-blade tool was coupled with the common horn model. The relationship between the length, thickness, edge angle, and width of the ultrasonic straight-blade tool and the resonant frequency of the system were given, which could be utilized to determine the structure parameters of ultrasonic straight tool system with changes in the boundary conditions. The proposed method was verified via experiments and it was beneficial to the resonance frequency design of the ultrasonic straight-blade tool with a higher accuracy than the constant cross-sectional model.

(2) The vibration model of the ultrasonic straight-blade tool and the coupling model of the tool and horn were fitted and achieved via a combination of trigonometric functions, making it convenient for designing the ultrasonic system with straight-blade tools. For ultrasonic systems, the presented model could be utilized to calculate the amount of change in the resonant frequency when assembled with straight-blade tools and the corrections that should be made on the system to maintain the resonant frequency.

(3) The error of the coupling model of tool and horn was analyzed and the error analysis was verified via experiments. When the resonant frequency of the system deviated from the basic frequency at which the model equation was constructed, then a systematic error had occurred and the systematic error increased while the deviation of the resonant frequency increased. When the resonant frequency of the system remained constant, the theoretical value calculated by the model could be in line with the actual value.

Funding The authors gratefully acknowledged the financial support for this research provided by the National Natural Science Foundation of China (Grant No. 51761145103 and Grant No. 51875311) and the Shenzhen Foundational Research Project (Subject Layout) (Grant No. JCYJ20160428181916222).

References

1. Yong L (1995) The development and application of the Nomex honeycomb in Russia Aerospace Area [J]. J Mater Eng 04 (in Chinese)
2. Fuzhong W, Jinyi L (2007) NC Machining process of honeycomb core part for aerospace [J]. Aeronautical Manufacturing Technology; 2007–07 (in Chinese)
3. Foo KCC, Chai GB, Seah LK (2007) Mechanical properties of Nomex material and Nomex honeycomb structure [J]. Compos Struct 80(4):588–594
4. Jie LI (2012) Research on high-speed milling Nomex paper-based honeycomb material with interlocked cutter [D]. Dalian University of Technology, Dalian
5. Huang X (2015) Research on ultrasonic cutting mechanism of Nomex honeycomb composites based on fracture mechanics [J]. J Mech Eng 51(23):205
6. Zhang HC, Gong Q (2012) Contrast on ultrasonic cutting and traditional NC machining for Nomex honeycomb sandwich component [C]. In: the 17th National Conference on Composite Materials, pp 160–164
7. Ahmad S, Zhang J, Feng P, Dingwen Y, Zhijun W, Ma K (2020) Processing technologies for Nomex honeycomb composites (NHCs): a critical review [J]. Compos Struct 112545. https://doi.org/10.1016/j.compstruct.2020.112545
8. Kumar J (2013) Ultrasonic matching-a comprehensive review [J]. Mach Sci Technol 17(3):325–379
9. Hu XP, Chen SY, Zhang ZC (2012) Research on curved surface forming of Nomex honeycomb material based on ultrasonic NC cutting [J]. Adv Mater Res 538-541:1377–1381
10. Liu E, Hu XP, Yu BH (2014) Research and development of ultrasonic CNC cutting path generation system for Nomex composite materials [J]. Adv Mater Res 941-944:1968–1972
11. Tony Atkins. The science and engineering of cutting [M]. 2009
12. Dammous S, Gilles R (2011) Use of ultrasonic straight blade in orthognathic surgery: review of 75 patients [J]. Int J Oral Maxillofac Surg 40(10):1082
13. Wang FJ, Zhang HJ, Liang CM, Tian YL, Zhao XY, Zhang DW (2015) Note: decoupling design for high frequency piezoelectric ultrasonic transducers with their clamping connections. Rev Sci Instrum 86(12):126111
14. Shung KK, Zippuro M (1996) Ultrasonic transducers and arrays [J]. IEEE Eng Med Biol 15(6):20–30
15. Yadava V, Deoghare A (2008) Design of horn for rotary ultrasonic machining using the finite element method [J]. Int J Adv Manuf Technol 39(1–2):9–20
16. Vivekananda K, Arka GN, Sahoo SK (2014) Design and analysis of ultrasonic vibratory tool (UVT) using FEM, and experimental study on ultrasonic vibration-assisted turning (UAT) [J]. Proc Eng 97: 1178–1186
17. Papakyriacou M, Mayer H, Fuchs U, Stanzl-Tschegg SE, Wei RP (2010) Influence of atmospheric moisture on slow fatigue crack growth at ultrasonic frequency in aluminium and magnesium alloys [J]. Fatigue Fract Eng Mater Struct 25(8–9):795–804
18. Zhou H, Zhang J, Feng P, Yu D, Cai W, Wang J (2020) Performance evaluation of a giant magnetostrictive rotary ultrasonic machine tool [J]. Int J Adv Manuf Technol 106(9-10):1–15
19. Cai WC, Zhang JF, Feng PF, Yu DW, Wu ZJ (2016) A bilateral capacitance compensation method for giant magnetostriction ultrasonic processing system [J]. Int J Adv Manuf Technol 90(9–12):1–9
20. Cai WC, Feng PF, Zhang JF, Wu ZJ, Yu DW (2016) Effect of temperature on the performance of a giant magnetostrictive ultrasonic transducer [J]. J Vibroeng 18(2):1307–1318
21. Zhang H, Wang F, Zhang D, Wang L, Xi T (2015) A new automaticresonant frequency tracking method for piezoelectric ultrasonic transducers used in thermosonic wire bonding [J]. Sensors Actuators A Phys 235:140–150
22. Zhen Y, Zhongning G, Yongjun Z, Weitao Z (2013) Research on frequency tracking in rotary ultrasonic machining [J]. Mach Tool Hydraul 6(8):556–560

23. Takasaki M, Maruyama Y, Mizuno T (2007). Resonant frequency tracing system for Langevin type ultrasonic transducers [C] Mechatronics and Automation, 2007. ICMA 2007. International Conference on. IEEE, 2007
24. Xin WU, Zhigang D, Renke K, Xianglong Z, Yidan W, Jinting L. Effect of shape parameters of straight blade cutter on performance of ultrasonic assisted cutting system [J]. Aeronautical Manufacturing Technology, 2016–22. https://doi.org/10.16080/j.issn1671-833x.2016.22.052 (in Chinese)
25. Zhou S, Yao Z, Sha J (2013) Dynamics analysis and structural optimization design of an ultrasonic cutter [J]. Chin Mech Eng 24(12):1631–1635
26. Yun-Dian Z, Jian C, Rui C, Chang-Shuai D (2017) Structural design of wide edge ultrasonic cutter [J]. J Mech Electr Eng. https://doi.org/10.3969/j.issn.1001-4551.2017.12.003 (in Chinese)
27. Hu XP, Dong XD, Yu BH (2016) Method of optimal design with SVR-PSO for ultrasonic cutter assembly [J]. Proc CIRP 50:779–783
28. Thomson WT (1972) Theory of vibration with applications [M]. Prentice-Hall, Upper Saddle River